Fiber-coupled nanowire photon counter at 1550 nm with 24% system detection efficiency

Fiber-coupled nanowire photon counter at 1550 nm with 24% system detection efficiency

Xiaolong Hu,[1,2] Tian Zhong,[1] James E. White,[1] Eric A. Dauler,[1] Faraz Najafi,[1] Charles H. Herder,[1] Franco N. C. Wong,[1] and Karl K. Berggren[1,3]

[1]*Research Laboratory of Electronics, Massachusetts Institute of Technology, 77 Massachusetts Avenue, Cambridge, Massachusetts 02139, USA*
[2] *xlhu@mit.edu*
[3] *berggren@mit.edu*

Received July 14, 2009; revised October 9, 2009; accepted October 15, 2009; posted October 29, 2009 (Doc. ID 114175); published November 17, 2009

We developed a fiber-coupled superconducting nanowire single-photon detector system in a close-cycled cryocooler and achieved 24% and 22% system detection efficiencies at wavelengths of 1550 and 1315 nm, respectively. The maximum dark count rate was ~1000 counts/s. © 2009 Optical Society of America

OCIS codes: 030.5260, 040.3060, 040.5160, 040.5570.

Superconducting nanowire single-photon detectors (SNSPDs, also referred to as SSPDs) [1] are an emerging IR photon-counting technology that can enable applications such as fiber-based long-haul quantum key distribution [2]. High speed, precise timing jitter, good device efficiency, and low dark count rate are among the potential advantages of SNSPDs over commercially available InGaAs/InP avalanche photodiode photon counters working in the Geiger mode. However, in contrast to avalanche photodiodes using only thermoelectric cooling, SNSPDs require cryogenics. Our group has demonstrated an SNSPD with a device efficiency of 57% at 1550 nm [3], but in that case the system detection efficiency was low because of inefficient coupling. Efficiently coupling light into SNSPDs remains a technical challenge for two reasons. First, efficient coupling requires a larger active area; however, constrictions limit the device efficiency of large-area devices [4]. Second, SNSPDs work at a cryogenic temperature of 4 K or below, which makes optical coupling more difficult than at room temperature. Consequently, the highest system detection efficiency reported for a single detector so far is still ~10% with a dark count rate of 10^5 counts/s (cps) when the detector was fully biased [5]. By putting four small SNSPDs together, 25% system detection efficiency and a dark count rate of 800 cps were achieved [6], but this configuration required bias and readout hardware for each element, thus complicating the electronics and packaging. Therefore, simultaneous high system detection efficiency and low dark count rate in a single-element SNSPD remains a major challenge to the field that this Letter addresses.

We demonstrated a fiber-coupled SNSPD system consisting of a single element in a close-cycled cryocooler. By integrating an optical cavity on the detector [3] and performing *in situ* optical alignment, we achieved system detection efficiencies of 24% and 22% at telecom wavelengths of 1550 and 1315 nm, respectively, with maximum dark count rate of ~1000 cps, as shown in Fig. 1. This high system detection efficiency and low dark count rate will permit many experiments in quantum optics at technologically interesting IR wavelengths.

Figure 2 shows a schematic of the chip package and a photograph of the core of the chip package, the chip plate. On the chip plate were mounted the SNSPD chip, a temperature sensor, three nanopositioners, a fiber focuser, and an SMA connector. The chip plate was mounted by screws to a hollow aluminum cylinder (the connector). The connector was then screwed onto the cold head. In this way, the detector was sitting in an enclosed metallic chamber facing the cold head. In the chamber was a small hole under the chip to permit bottom illumination from the fiber focuser. The detector was wire bonded directly to the SMA connector, which was connected by a semirigid coaxial cable that was itself heatsunk by being wrapped and taped around the connector and the second and first stages of the cryocooler. We used semirigid aluminum foil as the radiation shield for the chip package. This shield was clamped conformably to the first stage of the cryocooler by using a steel hose clamp. The resulting temperature was ~20 K at the radiation shield and 2.7 K at the chip plate.

To efficiently couple light to the SNSPD, one needs to maximize the overlap between the spatial mode of the light and the detector. This overlap is determined by the size of the detector relative to the size of the optical mode, and the relative alignment of the detec-

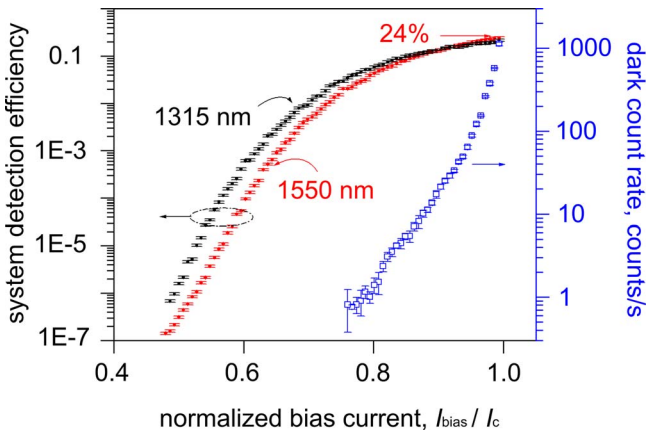

Fig. 1. (Color online) System detection efficiency and dark count rate versus normalized bias current, I_{bias}/I_c. I_c was 14.6 μA at 2.7 K. See text for details.

0146-9592/09/233607-3/$15.00

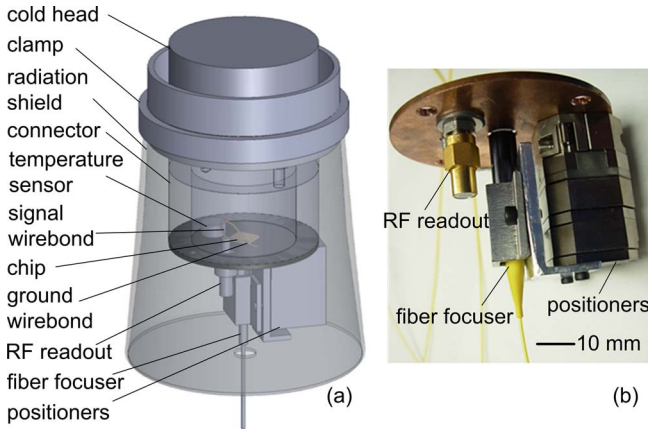

Fig. 2. (Color online) (a) Schematic of the chip package and (b) a photograph of the chip plate. In (a), the semirigid radiation shield and the aluminum connector were drawn to be semitransparent in order to make the chip inside visible. A semirigid coaxial cable (not shown) was wrapped and taped around the connector and the cold head.

tor with the optical beam. In our system, we used the fiber focuser to shrink the beam waist (full width at $1/e^2$ of the intensity profile) of the light from the single-mode fiber down to 5 μm, and we used our standard process [3] to fabricate a circular SNSPD with a diameter of 9 μm, as shown in Fig. 3. The width of the nanowire was ~100 nm, and the pitch of the meander was 200 nm. The large active area relative to the beam waist ensured that more than 99% of the incident light could overlap the detector if there were perfect alignment between the beam and the detector, and a lossless fiber focuser. This situation also provides some, but not complete, tolerance to mechanical vibration of the optical system relative to the detector. Although the total length of this single nanowire was similar to the overall length of four nanowires in the four-element detector used in [6], in the present case a defect on the nanowire would constrict the entire device and thus limit its overall efficiency. In the multielement detector, a single constriction would affect only one element out of four. Therefore, fabricating a uniform defect-free nanowire is more critical to the performance of this single-element configuration. The circular design minimized the length of the nanowire needed to cover a given area while maximizing coupling to the optical mode. Reduction of the total length of the nanowire offered two advantages: (1) a faster detector, because the speed of the detector is inversely proportional to its length [7], meaning that compared with a 9 μm $\times$9 μm square design, the speed of this circular detector is expected to be 1.16 times faster because the length of its nanowire is 1.16 times shorter; and (2) a decreased probability of constrictions, which are one of the limits of the device efficiency [4]. The total length of the nanowire was approximately 371 μm, and the FWHM of the resulting voltage pulse after amplification was ~5 ns. The reset time τ, defined as the time for the recovery of the detection efficiency to 90% of its initial value after a detection event [7], was expected to be approximately 25 ns according to our calculation based on [7]. We integrated the NbN meander with a microcavity on top as shown in the inset of Fig. 3 to enhance the optical absorption [3] so that we obtained 30% device efficiency [3] at 1550 nm, measured by using a probing station at 2.1 K. The 0.6 K temperature difference between the probing station and the cryocooler did not make an observable difference in critical current, and therefore we assume that the maximum device efficiency was also 30% in the cryocooler.

The nanopositioners (two ANPx101 and one ANPz101, all from Attocube System) in our setup shown in Fig. 2 allowed us to precisely control *in situ* the three-dimensional position of the beam waist. The fiber focuser was clamped into a V groove, mounted on the nanopositioner stack. When voltage pulses were applied, the nanopositioners performed stick–slip motion with a step size as small as ~10 nm at 2.7 K. We scanned the beam three dimensionally until we found the maximum of the photon count signal.

The maximum dark count rate measured when we increased the bias current up to 99% of the critical current was ~1000 cps, as shown in Fig. 1. We took a number of steps to minimize the counts resulting from stray light coupled into the detector. The chip package was designed so that the chip could only be illuminated from the back by the fiber focuser. The chip was sitting in the middle of the chip plate and was glued to the plate by conductive silver paint, which provided thermal contact. The entire chip package, including the nanopositioner stack and the fiber focuser, was enclosed in the radiation shield. The fiber entered the radiation shield through a hole with a diameter of 8 mm and connected with the fiber outside the chamber through a vacuum feedthrough.

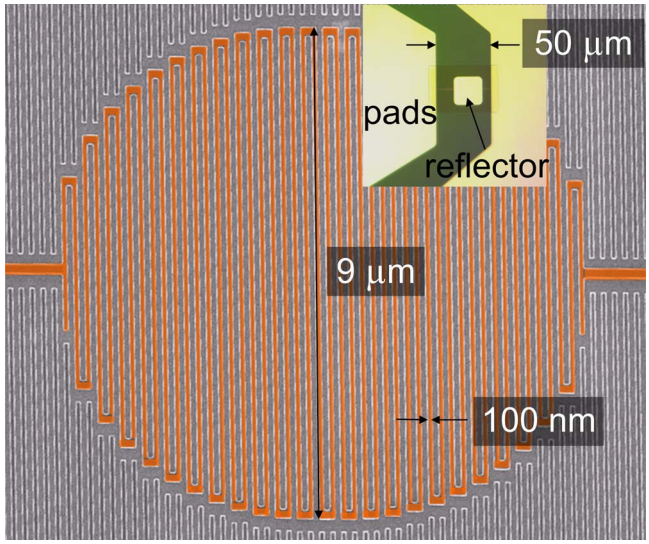

Fig. 3. (Color online) Scanning electron micrograph of a circular superconducting nanowire single-photon detector with a diameter of 9 μm before a gold reflector was placed on top. The width of the wire was ~100 nm. The nanowire detector itself is colored. The linear structures surrounding the detector were used for improving electron dose uniformity in scanning-electron-beam lithography. Inset, plan-view optical micrograph of the detector after integration of a cavity and a gold reflector.

We then covered this 8-mm diameter hole with aluminum foil. The piece of fiber outside the cryocooler was in a metal jacket, and when we measured the dark count rate, we capped the FC/PC fiber connector at the end with a metal cap. We also used aluminum foil to cover the two quartz windows of the cryocooler to prevent the stray light from leaking into the fiber. With all of these strategies, the dark count rate that we measured was ~150 cps and ~1000 cps when we biased the detector at 96% and 99%, respectively, of the critical current I_c, which was 14.6 μA in our case. For comparison, without covering the quartz window or the FC/PC fiber connector, the dark count rate was above 2000 cps when we biased the detector at 99% of its I_c.

We used an attenuated laser as a light source to measure the system detection efficiency. The optical path consisted of a laser, a precision attenuator, a polarization controller, and the fiber focuser, all of which were connected by single-mode fibers. Before adding attenuation, we used an optical power meter to measure the optical power P (in watts) coming out of the polarization controller. We controlled this power to be about 100 μW, and added attenuation A (in decibels), which was usually 100 dB. Therefore, the flux of photons was about 10^5 photons/s, which was much larger than the dark count rate and much smaller than the maximum counting rate of the detector, $\sim 1/\tau$, which was ~40 MHz. Because the response of the detector was polarization dependent [8], we maximized the counts by adjusting the polarization with the polarization controller. The ratio of the maximum to minimum counting rate due to polarization variation was measured to be ~2 at both 1550 and 1315 nm wavelengths. This ratio is primarily determined by the filling factor of the meander [8], which was 50% in our device. The output voltage pulses of the detector after 50 dB amplification by three RF amplifiers were counted by a photon counter. If the counting rate is denoted N and the wavelength of the light is denoted λ, the system detection efficiency η is simply calculated as $\eta = 10^{0.1A} hcN/(P\lambda)$, in which h is Plank's constant and c is the speed of light in vacuum. In this way, the system detection efficiencies at wavelengths of 1550 and 1315 nm were determined, as shown in Fig. 1, as a function of bias current. At a bias at 99% of I_c, the system detection efficiency reached its maximum of 24% for 1550 nm and 22% for 1315 nm. We repeated the measurement of total counts and dark counts five times, and the efficiency and dark count rate shown on the figure were obtained by averaging. The error for the efficiency measurement was calculated assuming ±0.1 dB uncertainty in the precision attenuator, ±5% uncertainty in the optical power meter, and one standard deviation (SD) of the observed fluctuation in counting rate, which we believe was due to the intensity fluctuation of the laser, coupling efficiency fluctuation induced by the mechanical vibration of the piston, and intrinsic shot noise. These errors were summed in quadrature. At a bias at 99% of I_c, the resulting maximum system detection efficiencies were 24% ± 1% and 22% ± 1% at wavelengths of 1550 and 1315 nm, respectively. The error of the dark count rate in Fig. 1 was taken to be the SD of the measurements. The SD for dark counts was consistent with the expected fluctuation due to shot noise.

By comparing the device efficiency to the system detection efficiency, we estimated the coupling efficiency to be ~80%. We hypothesize two reasons for this incomplete coupling: (1) optical loss in the fiber focuser, which was measured to be 10% at room temperature, and (2) the dynamic misalignment between the beam and the detector resulting from mechanical vibration induced by the cryocooler. However, the major factor limiting the system detection efficiency was still the device efficiency, meaning that the absorptance of the NbN nanowire was not 100%, and small constrictions limited the internal detection efficiency (the probability of resistive state formation after absorbing one photon). To further enhance the device efficiency of a large-area SNSPD, it will be important to increase the optical absorptance of the NbN nanowire [9] and improve the quality of the NbN film.

We thank J. M. Daley, M. K. Mondol, and Dr. A. J. Kerman for help and thank Prof. G. Gol'tsman and Dr. B. Voronov for supplying the unpatterned NbN film on sapphire substrate. Patterning of the detector was done in MIT's shared scanning-electron-beam lithography. One of the authors, E. A. Dauler, is now with MIT Lincoln Laboratory. This work was sponsored by IARPA and by the United States Air Force under Air Force contract FA8721-05-C-0002.

References

1. G. N. Gol'tsman, O. Okunev, G. Chulkova, A. Lipatov, A. Semenov, K. Smirnov, B. Voronov, A. Dzardanov, C. Williams, and R. Sobolewski, Appl. Phys. Lett. **79**, 705 (2001).
2. H. Takesue, S. W. Nam, Q. Zhang, R. H. Hadfield, T. Honjo, K. Tamaki, and Y. Yamamoto, Nat. Photonics **1**, 343 (2007).
3. K. M. Rosfjord, J. K. W. Yang, E. A. Dauler, A. J. Kerman, V. Anant, B. M. Voronov, G. N. Gol'tsman, and K. K. Berggren, Opt. Express **14**, 527 (2006).
4. A. J. Kerman, E. A. Dauler, J. K. W. Yang, K. M. Rosfjord, K. K. Berggren, G. Gol'tsman, and B. Voronov, Appl. Phys. Lett. **90**, 101110 (2007).
5. A. Korneev, Y. Vachtomin, O. Minaeva, A. Divochiy, K. Smirnov, O. Okunev, G. Gol'tsman, C. Zinoni, N. Chauvin, L. Balet, F. Marsili, D. Bitauld, B. Alloing, L. Li, A. Fiore, L. Lunghi, A. Gerardino, M. Halder, C. Jorel, and H. Zbinden, IEEE J. Sel. Top. Quantum Electron. **13**, 944 (2007).
6. E. A. Dauler, A. J. Kerman, B. S. Robinson, J. K. W. Yang, B. Voronov, G. Gol'tsman, S. A. Hamilton, and K. K. Berggren, J. Mod. Opt. **56**, 363 (2009).
7. A. J. Kerman, E. A. Dauler, W. E. Keicher, J. K. W. Yang, K. K. Berggren, G. N. Gol'tsman, and B. M. Voronov, Appl. Phys. Lett. **88**, 111116 (2006).
8. V. Anant, A. J. Kerman, E. A. Dauler, J. K. W. Yang, K. M. Rosfjord, and K. K. Berggren, Opt. Express **16**, 10750 (2008).
9. X. Hu, C. W. Holzwarth, D. Masciarelli, E. A. Dauler, and K. K. Berggren, IEEE Trans. Appl. Supercond. **19**, 336 (2009).